DALTON
FULL PAPER

A new redox-responsive 14-membered tetraazamacrocycle with ferrocenylmethyl arms as receptor for sensing transition-metal ions

Judite Costa,[a,b] Rita Delgado,[a,c] Michael G. B. Drew,[d] Vitor Félix[a,e] and André Saint-Maurice[a]

[a] *Instituto de Tecnologia Química e Biológica, UNL, Apartado 127, 2781-901 Oeiras, Portugal*
[b] *Faculdade de Farmácia de Lisboa, Av. das Forças Armadas, 1600 Lisboa, Portugal*
[c] *Instituto Superior Técnico, Dep. de Química, Av. Rovisco Pais, 1049-001 Lisboa, Portugal*
[d] *Department of Chemistry, University of Reading, Whiteknights, Reading, UK RG6 6AD*
[e] *Dep. de Química, Universidade de Aveiro, 3810-193 Aveiro, Portugal*

Received 3rd February 2000, Accepted 26th April 2000
Published on the Web 26th May 2000

A new redox-responsive receptor, 3,11-bis(ferrocenylmethyl)-7-methyl-3,7,11,17-tetraazabicyclo[11.3.1]-heptadeca-1(17),13,15-triene, L^1, has been synthesized. The protonation constants of this compound and the stability constants of its complexes with Ni^{2+}, Cu^{2+}, Zn^{2+}, Cd^{2+}, and Pb^{2+} were determined at 25.0 °C, in methanol–water (1 : 1, v/v), and at ionic strength 0.10 mol dm^{-3} in KNO_3. The values of the protonation constants of L^1 are similar to those of the parent macrocycle, 7-methyl-3,7,11,17-tetraazabicyclo[11.3.1]heptadeca-1(17),13,15-triene L^2, except for K_2 which is 1.82 log units lower than that of L^2. Structural reasons are proposed to explain this behaviour. The stability constants of the metal complexes of L^1 are lower than those of L^2 as expected on the basis of its lower overall basicity, but the Cd^{2+} complex is exceptional exhibiting a higher stability for L^1. The complexation of L^1 with different metals shifts anodically the ferrocene–ferrocenium half-wave potential in relation to that of the free compound, the largest shift being observed for Cu^{2+}, followed by Ni^{2+}, and then Zn^{2+} and Cd^{2+}. No shift was observed for Pb^{2+}. It was verified that L^1 is a copper-selective sensor in the presence of Ni^{2+}, Zn^{2+}, Cd^{2+} and Pb^{2+} and although it is not the first compound for which this property is claimed it is probably the easiest to synthesize. The electronic spectra of $[CuL^1]^{2+}$ reveal that the four nitrogen atoms of the macrocycle form a square-planar arrangement with a pronounced tetrahedral distortion. The single crystal structures of $[CuL^1Cl][CuL^1I]Cl_2\cdot 1.25H_2O$ **1** and $[ZnL^1I]Cl\cdot 2H_2O$ **2** have shown that these complex cations have distorted square pyramidal co-ordination spheres, the basal being planes formed by the four nitrogen atoms of the macrocyclic framework in **1a**$^+$ and **1b**$^+$ while in **2**$^+$ it is defined by three nitrogen atoms of L^1 and one iodine atom. The apical positions are occupied by a chlorine atom in **1a**$^+$ and by an iodine atom in **1b**$^+$, and by the nitrogen donor atom of the macrocycle *trans* to the pyridine ring in complex **2**$^+$. To achieve the geometric arrangement described for **2**$^+$ the macrocycle folds considerably through the line defined by the two nitrogen atoms contiguous to the pyridine group. It was also found that the intramolecular distances between the ferrocene groups and transition metal receptor centres studied play an important role in the redox behaviour of these complexes.

Introduction

In the last decade a number of redox-responsive receptors for the recognition of metal ions[1–16] as well as other cationic[17] and anionic[18–21] substrates have been designed and studied. Some of these are not only redox-responsive molecules but also selective to specific substrates, allowing their detection among other chemically similar cations or anions. These systems recognise electrochemically the binding of the substrate through space interactions or through bond linkages between the receptor site and the redox centre.[1] Different redox-active units have been attached in close proximity to the co-ordination site, the most common of them being ferrocenyl groups, and different molecules have been designed to recognise the substrate or guest, among them specific macrocycles which provide selectivity, *e.g.* crown ethers for alkali, alkaline-earth metal and ammonium cations, or polyaza and polyoxapolyaza macrocycles for transition-metals and anions. In this way, co-operation between the macrocycle and the attached ferrocene–ferrocenium redox couple results in a switch, turning off the recognition ability by oxidation, due to the formation of the charged ferrocenium cation and the consequent decrease of the association ability between the receptor (macrocycle) and the substrate. Subsequently the switch can be turned back on by reduction to ferrocene and recovery of the complexing ability of the macrocycle for the guest.

In our search for redox-responsive selective receptors for toxic metal ions we prepared the new compound L^1, and carried out a systematic analysis of its behaviour on protonation and on complexation with the Ni^{2+}, Cu^{2+}, Zn^{2+}, Cd^{2+} and Pb^{2+} ions in solution and in the solid state, in order to investigate the causes of the extent of the anodic shift of the redox potential of the ferrocene–ferrocenium couple of L^1 by the association of protons or transition metal ions.

Experimental

Reagents

The parent macrocycle 7-methyl-3,7,11,17-tetraazabicyclo-[11.3.1]heptadeca-1(17),13,15-triene (L^2) was synthesized by previously reported procedures.[22,23] (Ferrocenylmethyl)-trimethylammonium iodide was prepared according to literature procedures.[24,25] All the chemicals were of reagent grade and used as supplied without further purification. The reference used for the ^{1}H NMR measurements in D_2O was sodium 3-(trimethylsilyl)propanoate and in $CDCl_3$ the solvent itself.

DOI: 10.1039/b000938p

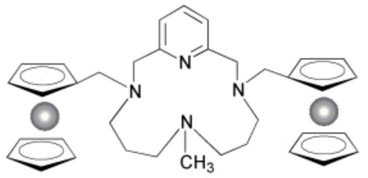

L^1

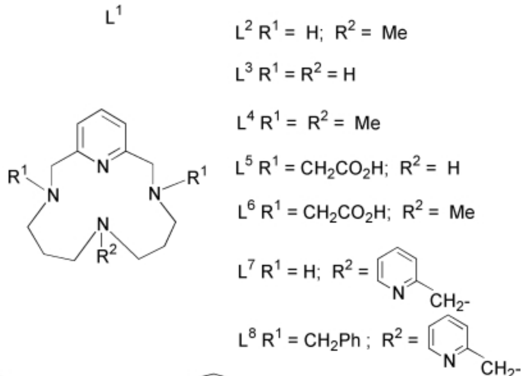

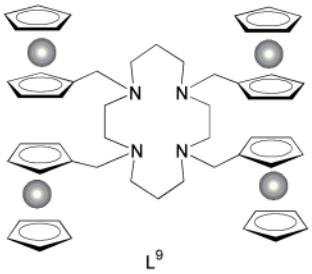

L^9

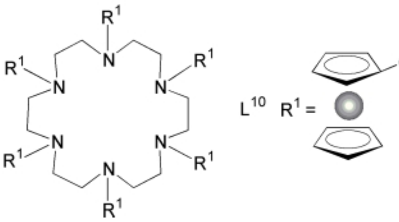

Syntheses

3,11-Bis(ferrocenylmethyl)-7-methyl-3,7,11,17-tetraazabicyclo[11.3.1]heptadeca-1(17),13,15-triene (L^1). The compound L^2 (0.45 g, 1.8 mmol) was dissolved in dry acetonitrile (20 cm^3) and (ferrocenylmethyl)trimethylammonium iodide (1.410 g, 3.6 mmol) added in small portions. The resulting mixture was refluxed for 3 h, the precipitate was filtered off, the solvent evaporated and the residue dissolved in dichloromethane (100 cm^3). This solution was washed with several portions of water (5 × 100 cm^3). The organic phase was dried with $MgSO_4$, filtered, and evaporated to dryness. The yellow oil obtained was purified by silica column chromatography using first dichloromethane, then dichloromethane–acetone (96:4, v/v) and finally mixtures of dichloromethane–methanol with increasing amounts of methanol (5 to 20%). The dark yellow compound eluted in the final fractions, after evaporation of the solvent, was verified to be the diprotonated form of the desired macrocycle, $[H_2L^1]ClI$. Yield: 75%. ^1H NMR ($CDCl_3$): δ 2.06 (4 H, q, $NCH_2CH_2CH_2N$), 2.88 (4 H, t, NCH_2CH_2), 2.93 (3 H, s, NCH_3), 3.27 (4 H, t, NCH_2CH_2), 3.62 (4 H, s, NCH_2), 3.78 (4 H, s, NCH_2), 4.16 (10 H, s, ferrocene), 4.20 (8 H, m, ferrocene), 7.12 (2 H, d, pyridine) and 7.69 (1 H, t, pyridine). ^{13}C NMR ($CDCl_3$): δ 19.0, 38.2, 49.0, 52.3, 55.0, 56.3, 66.3, 67.9, 78.7, 120.5, 135.3 and 154.8. FAB: *m*/*z* 645, MH^+. Found: C, 52.1; H, 5.7; N, 6.5%. Calc. for $C_{36}H_{46}ClFe_2IN_4\cdot H_2O$: C, 52.3; H, 5.9; N, 6.8%. The number of acidic protons of the isolated compound was confirmed by an acid–base titration and the presence of the halogens by qualitative tests.

The prepared compound, $[H_2L^1]ClI$, was dissolved in $CHCl_3$ and an aqueous solution of NaOH added. The aqueous solution containing the halogens was separated and iodine formed by addition of H_2O_2, which was removed by extraction with $CHCl_3$. The presence of chloride in the aqueous solution was confirmed by the precipitation of AgCl by addition of $AgNO_3$. The product which remained in the initial organic phase was the desired pure compound L^1, mp 157–158 °C. Found: C, 65.6; H, 7.0; N, 8.5%. Calc. for $C_{36}H_{44}Fe_2N_4\cdot H_2O$: C, 65.3; H, 7.0; N, 8.5%.

Complex $[CuL^1Cl][CuL^1I]Cl_2\cdot 1.25H_2O$ 1. An aqueous solution of $Cu(NO_3)_2\cdot 6H_2O$ (1.27 × 10^{-4} mol, 0.047 g) was added to a stirred solution of $[H_2L^1]ClI$ (1.28 × 10^{-4} mol, ≈0.10 g) dissolved in the minimum volume of methanol (≈2 cm^3). The mixture was stirred for 2 h and then concentrated to dryness. The residue was taken up in methanol. Dark blue crystals were formed in two days by slow evaporation of the solvent in contact with air. Yield: ≈90%.

Complex $[ZnL^1I]Cl\cdot 2H_2O$ 2. The complex was prepared by the procedure used for the copper(II) complex, but $Zn(NO_3)_2$ was used. The yellow crystals were formed in three days by slow evaporation of the solvent. Yield: ≈90%.

Complex $[NiL^1Cl]Cl$ 3. This complex was prepared by the procedure used for the copper(II) complex, but $Ni(NO_3)_2$ was used. Green crystals were formed in three days by slow evaporation of the solvent. Yield: ≈90%.

Potentiometric measurements

Reagents and solutions. Metal ion solutions were prepared at about 0.025 mol dm^{-3} from the nitrate salts of the metals, of analytical grade with demineralised water (obtained by a Millipore/Milli-Q system) and were standardised as described.[26] A carbonate-free solution of the titrant, NaOH, was freshly prepared in methanol–water (1:1, v/v) solution, maintained in a closed bottle, and discarded when the percentage of carbonate was about 0.5% of the total amount of base (tested by Gran's method).[27] The support electrolyte, KNO_3, was also prepared in methanol–water (1:1, v/v) solution.

Equipment and working conditions. The equipment used was described before.[26] The glass electrode was pre-treated by soaking it in methanol–water (1:1, v/v) solution for a week, in order to prevent erratic responses. The temperature was kept at 25.0 ± 0.1 °C; atmospheric CO_2 was excluded from the cell during the titration by passing purified argon across the top of the experimental solution in the reaction cell. The ionic strength of the solutions was kept at 0.10 mol dm^{-3} with KNO_3.

Measurements. The [H$^+$] of the solutions was determined by measurement of the electromotive force of the cell, $E = E'^{\circ} + Q \log [H^+] + E_j$; E'°, Q, E_j and $K'_w = [H^+][OH]$ were obtained as described previously.[26] The term pH is defined as $-\log [H^+]$. The value of K'_w for the solvent used was found equal to $10^{-13.91}$ mol^2 dm^{-6} under our experimental conditions, in agreement with that determined by Rochester.[28]

The potentiometric equilibrium measurements were made on 20.00 cm^3 of ≈2.50 × 10^{-3} mol dm^{-3} ligand solutions diluted to a final volume of 30.00 cm^3, in the absence of metal ions and in the presence of each metal ion for which the $C_M : C_L$ ratios were 1:1 and 2:1. A minimum of two replicates were performed. A correction was made for the small decrease in volume which occurs on mixing methanol and water. Care has been taken to maintain unaltered the methanol:water ratio in the measured solution.

Calculation of equilibrium constants. Protonation constants $K_i^H = [H_iL]/[H_{i-1}L][H]$ were calculated by fitting the potentiometric data obtained for the "free" ligand using the HYPER-

QUAD program.[29] Stability constants of the various species formed in solution were obtained from the experimental data corresponding to the titration of solutions of different metal ion to ligand ratios, also using the HYPERQUAD program. The initial results were obtained in the form of overall stability constants, $\beta_{M_mH_hL_l} = [M_mH_hL_l]/[M]^m[L]^l[H]^h$. Only mononuclear species, ML, M(HL) and M(H_{-1}L) [where $\beta_{M(H_{-1}L)} = \beta_{ML(OH)} \cdot K_W$], were found. Differences, in log units, between the values $\beta_{M(HL)}$ [or $\beta_{M(H_{-1}L)}$] and β_{ML} provide the stepwise protonation reaction constants, shown in the tables below. The errors quoted are the standard deviations of the overall stability constants given directly by the program for the input data which include all the experimental points of all titration curves. The standard deviations of the stepwise constants were determined by the normal propagation rules.

The protonation constants were obtained from 120 experimental points (3 titration curves) and the stability constants for each metal ion were determined from 70 to 120 experimental points (2 to 4 titration curves). First, each titration curve of a given system was treated separately and finally the data of all the titration curves were merged and treated simultaneously to give the values of stability constants.

Spectroscopic studies

^{1}H NMR spectra were recorded with a Bruker AMX-300 spectrometer at probe temperature. The electronic spectra of the complexes prepared by the addition of the metal ion (in the form of the nitrate salt) to the ligand at the appropriate pH value (corresponding to the total formation of the metal complex) were recorded with a UNICAM UV-vis spectrophotometer model UV-4, in acetonitrile, DMF and methanol–water (1 : 1, v/v). EPR spectroscopy measurements were made with a Bruker ESP 380 spectrometer equipped with a continuous-flow cryostat for liquid nitrogen, operating at X-band. The spectra of the Cu^{2+} complexes, $\approx 2.0 \times 10^{-3}$ mol dm^{-3}, were recorded at 129 K in methanol and DMF. Computer simulations of the spectra were carried out with a program for a micro computer.[30]

Electrochemistry

The electrochemical instrumentation consisted of a BAS CV - 50W Voltammetric Analyzer connected to BAS/Windows data acquisition software. All the electrochemical experiments were run under argon at room temperature. Tetrabutylammonium nitrate (Aldrich) was used as supporting electrolyte; it was recrystallised from ethanol. Cyclic voltammetry experiments were performed in a glass cell MF-1082 from BAS in a C-2 cell enclosed in a Faraday cage. The reference electrode was Ag–AgCl (MF-2079 from BAS) and its potential was −44 mV relative to the SCE. The reference electrode was calibrated with a solution of ferrocene (1 mmol dm^{-3}) to obtain a potential in agreement with the literature value.[31] The auxiliary electrode was a 7.5 cm platinum wire (MW-1032 from BAS) with a gold-plated connector. The working electrode was a platinum disk (MF-2013 from BAS) *ca.* 0.022 cm^2 sealed in Kel-F plastic. Between each CV scan the working electrode was electrocleaned, polished on Diamond 1uM and alumina, cleaned with water–methanol and sonicated before use, according to standard procedures. Solvents were dried before use. The solutions of the receptor or of the complexes (1.2×10^{-3} to 6.0×10^{-3} mol dm^{-3}) in dry acetonitrile were previously prepared in tetrabutylammonium nitrate (0.1 mol dm^{-3}). For studies of increasing amount of guest, a solution was prepared of the receptor in acetonitrile (in tetrabutylammonium nitrate 0.1 mol dm^{-3}) and the guest added as a 0.1 mol dm^{-3} solution using a micro-syringe.

Crystallography

The crystallographic data and pertinent structure refinement parameters for complexes $[CuL^1Cl][CuL^1I]Cl_2 \cdot 1.25H_2O$ **1** and $[ZnL^1I]Cl \cdot 2H_2O$ **2** are listed in Table 5. Crystal data of these two complexes and also of $[NiL^1Cl]Cl$ **3** (see below) were collected using graphite-monochromated Mo-Kα radiation ($\lambda = 0.71073$ Å) on a MAR research image plate system at Reading University. Crystals, mounted in a glass capillary, were positioned at 70 mm from the image plate. 95 Frames were measured at 2° intervals with a counting time suitable for the diffraction pattern exhibited by the complex under investigation. Data analysis was performed with the XDS program.[32] The intensities of the three complexes were corrected empirically for absorption effects with the DIFABS program,[33] using a version modified for the image plate system.

The structures were solved by direct methods and by subsequent Fourier difference syntheses and refined by full matrix least squares on F^2 using the SHELX 97 system programs.[34] Anisotropic thermal parameters were used for non-hydrogen atoms, except for oxygen atoms of water molecules and chlorine anions of complexes **1** and **2**, which were disordered. Thus these species were introduced in the refinement using disordered models comprising alternative positions with occupancies constrained to sum to appropriate integer values and with common isotropic thermal parameters. The C–H hydrogen atoms were introduced in the refinement at idealised positions with isotropic thermal parameters equal to 1.2 times those of the parent carbon atom. As would be expected, the hydrogen atoms of the water molecules of **1** and **2** were not discernible from Fourier difference maps and not included in the structure refinement. Molecular diagrams were drawn using the PLATON graphical package.[35]

CCDC reference number 186/1952.

See http://www.rsc.org/suppdata/dt/b0/b000938p/ for crystallographic files in .cif format.

Results and discussion

Syntheses of macrocyclic ligands

Following well established methods,[14,17] the reaction of the parent macrocycle L^2 and (ferrocenylmethyl)trimethylammonium iodide gave the compound L^1 in good yield after chromatographic purification. The synthesis proceeded without addition of a base, like sodium or potassium carbonate,[14,17] because $(CH_3)_3N$ was formed during the reaction. However, the synthesized compound was prepared originally in the protonated form, $[H_2L^1]ClI$, and it was necessary to add two more equivalents of base to isolate the desired compound. All the measurements, both potentiometric and voltammetric, were made with the compound L^1, but the single crystals of the different complexes used in the X-ray diffraction studies were obtained from $[H_2L^1]ClI$. In spite of our best efforts we were unable to crystallise the complexes prepared directly from L^1, even after addition of Cl^- or I^- to the solution. Compound L^1 is readily soluble in most of the organic solvents, but it was necessary to add 50% v/v of methanol in order to prepare a 2.5×10^{-3} mol dm^{-3} aqueous solution.

Protonation constants

In Table 1 are listed the protonation constants of L^1 determined at 25.0 °C and 0.10 mol dm^{-3} KNO_3 ionic medium obtained in methanol–water (1 : 1 v/v), and also for comparison the corresponding values of L^2 under the same conditions and in water. The values of protonation constants of macrocycles with small cavity sizes are mainly controlled by the repulsion of charges inside the cavity, due to the restricted movement imposed by the macrocyclic framework on the protonated positively charged ammonium centres to minimise repulsion, and by the possible formation of hydrogen bonds inside the cavity. Therefore a similar protonation sequence for L^1 and L^2 would be expected. For the latter, a ^{1}H NMR titration study[23] showed that the first

Table 1 Stepwise protonation (log K_i^{H}) constants of L^1 and L^2 determined at 25.0 °C in 0.10 mol dm^{-3} KNO_3 and methanol–water (1 : 1 v/v)

Equilibrium quotient	$L^{1\,a}$	$L^{2\,a}$	$L^{2\,b}$
[HL]/[L][H]	9.98(1)	9.60(2)	9.74
[H_2L]/[HL][H]	6.30(3)	8.12(3)	8.67
[H_3L]/[H_2L][H]	4.28(4)	3.95(4)	4.67
[H_4L]/[H_3L][H]	<2	<2	<1
[H_4L]/[L][H]^4	<22.6	<23.7	<24.1

[a] Values in parentheses are the standard deviations on the last significant figure. [b] Ref. 23, $I = 0.10$ mol dm^{-3} $NaNO_3$, in water.

two protonations of L^2 occur predominantly at nitrogen atoms contiguous to the pyridine, while the third protonation occurs mainly on the nitrogen opposite to the pyridine, and the last centre is only protonated at very low pH values. The values of the first two protonation constants of this compound are high as the nitrogen atoms involved are located in opposite positions, but the third one is decreased drastically because it corresponds to protonation on contiguous basic centres of the molecule, so a decrease of 4.00 log units is observed even though these centres are separated by propane chains.

As expected for compounds having the same protonation sequence, L^1 exhibits similar values for K_1 and K_3, but a surprising large difference of 1.82 log units exists between the second protonation constants, the N-ferrocenyl derivative L^1 having the lower value, and consequently a lower overall basicity. Therefore, the two compounds have different sequences of protonation, because in L^1 the second protonation is lower than expected and closer to the third one, and so protonation of the second and third centres is not sequential but almost simultaneous. This interesting fact might have a structural reason owing to the presence of the bulky ferrocenyl groups, restricting the mobility of the attached nitrogen atoms to a larger extent than hydrogen atoms of L^2, leading to a shorter separation of the positive charges formed, and so increasing the acidity of the second nitrogen of L^1. Unfortunately, it was impossible to obtain suitable single crystals for X-ray diffraction studies to confirm this point.

Martínez-Máñez and co-workers[9–12,14,16,20] have also studied the acid–base behaviour of some azamacrocycles with ferrocenylmethyl groups attached to all nitrogen atoms of the molecules[9,11,14,16] and also to open-chain polyazaalkane ferrocene-functionalised[12,20] and other ferrocenophanes.[10,12] However, the comparison with our case is not straightforward even for similar compounds, such as 1,4,8,11-tetra(ferrocenylmethyl)-1,4,8,11-tetraazacyclotetradecane, L^9, or 1,4,7,10,13,16-hexa(ferrocenylmethyl)-1,4,7,10,13,16-hexaazacyclooctadecane, L^{10}, because these compounds have more pendant ferrocenylmethyl groups and a lower relative permittivity solvent, thf–water (70 : 30 v/v), is used in the measurements.

Stability constants

The stability constants of L^1 with the metal ions studied in this work determined at 25.0 °C and 0.10 mol dm^{-3} KNO_3 in methanol–water (1 : 1 v/v) are listed in Table 2 together with those of the complexes of L^2 for comparison. Only mononuclear species were formed, ML and M(HL), but hydroxo complexes [ML(OH)] were also found in some systems. We have checked the possibility of formation of other species, but they are not formed under our experimental conditions. The stability constant for the copper(II) complex is very high, and it was determined with less accuracy because the complex is almost totally formed at the beginning of the titration. A more precise value would require a competitive method with a second ligand, but values of stability constants for ligands which would be able to compete with L^1 are not available in the medium used, therefore it would be necessary to study first the chosen ligand. However, for the required conclusions, the precision obtained is sufficient.

Table 2 Stability constants (log $K_{M_mH_hL_l}$) of the complexes of L^1 and $L^{2\,a}$ with some divalent metal ions determined at 25.0 °C in 0.10 mol dm^{-3} KNO_3 and methanol–water (1 : 1 v/v)

Ion	Equilibrium quotient	$L^{1\,b}$	L^2
Ni^{2+}	[ML]/[M][L]	16.90(4)	16.267[c]
Cu^{2+}	[ML]/[M][L]	19.1(1)	20.23
Zn^{2+}	[ML]/[M][L]	10.48(1)	11.91
	[M(HL)]/[ML][H]	4.05(2)	—
	[ML]/[ML(OH)][H]	8.23(2)	8.06
Cd^{2+}	[ML]/[M][L]	9.23(2)	8.77
	[M(HL)]/[ML][H]	4.78(4)	—
	[ML]/[ML(OH)][H]	10.67(5)	9.62
Pb^{2+}	[ML]/[M][L]	7.32(1)	9.029
	[ML]/[ML(OH)][H]	8.07(2)	—

[a] Ref. 23, $I = 0.10$ mol dm^{-3} $NaNO_3$, in water. [b] Values in parentheses are the standard deviations on the last significant figure. [c] Value for L^3, that for L^2 is not available; ref. 23.

The complexes of L^1 with the divalent first row-transition metals follow the Irving–Williams order of stability, with the maximum stability constant for Cu^{2+} as usual, but a very abrupt fall of the constants for the Zn^{2+} and Ni^{2+} complexes.

All the values of stability constants determined for the complexes of L^1 are similar to those of L^2, in spite of the medium differences. However the values of L^1 are always lower than those of L^2, as expected on the basis of the differences of the overall basicity of the two ligands, except for the Cd^{2+} complex for which the value for L^1 is higher than that of L^2. This exceptional value for the Cd^{2+} complex of L^1 is particularly significant and can only be ascribed to a higher co-ordination number or to stereochemical reasons. The macrocycle provides only four donor atoms, but Cd^{2+} can achieve higher co-ordination numbers using other ligands present in solution, such as Cl^-, Br^- or water. On the other hand, the structure of the zinc(II) complex presented below suggests that the same type of geometric arrangement, though possibly more distorted, may be adopted by the cadmium complex. Another case of remarkably high thermodynamic stability for the Cd^{2+} complex was recently found with a ligand derivative of the same macrocycle, L^2, with three N-methylpyridine pendant arms.[26] However the pendant arms of this latter ligand have donor atoms directly involved in the co-ordination to the metal, contrary to what happens in the case of L^1.

Electrochemistry

Good design of electrochemical sensors based on redox-responsive molecules requires that different metals cause a different shift of the redox potential. Therefore electrochemical investigation is a necessary prerequisite to test the performance of the new molecules.

Cyclic voltammograms of all systems studied exhibit one well defined reversible two-electron wave over a large pH range suggesting that the two ferrocene moieties become oxidised in one step. The compound L^1 displays a reversible oxidation process with separation of about 80 mV and with cathodic and anodic intensity ratios close to unity.

The redox potential of this molecule is pH-dependent. When the pH is decreased, by addition of a solution of HBF_4 in acetonitrile, a steady $E_{1/2}$ shift to more anodic potentials is observed as expected, because the formation of the charged ammonium groups in the macrocycle makes the oxidation of the Fe^{II} in the ferrocene more difficult. The difference found between the redox potential of the basic form of the ligand and after 1, 2 and 3 equivalents of acid added was 48, 65 and 80 mV, respectively, the increment being lower for each equivalent of

Table 3 Redox potentials of L^1 and its Ni^{2+}, Cu^{2+}, Zn^{2+}, and Cd^{2+} complexes[a]

	H^+	Ni^{2+}	Cu^{2+}	Zn^{2+}	Cd^{2+}
$E_{1/2}$/V	0.546 (1 equivalent) 0.562 (2 equivalents) 0.578 (3 equivalents)	0.594	0.608	0.567	0.564
$\Delta E_{1/2}{}^b$/mV	48 (1 equivalent) 65 (2 equivalents) 80 (3 equivalents)	91	111	66	57
$\log K_{ML(ox)}{}^c$	—	13.8	15.4	8.3	7.3

[a] All were recorded in acetonitrile at ambient temperature (≈293 K), 0.1 mol dm^{-3} NBu_4NO_3. All the $E_{1/2}$ values are relative to AgCl–Ag and accurate to ±5 mV. [b] $\Delta E_{1/2} = [E_{1/2}\,(\text{complex}) - E_{1/2}\,(\text{free receptor})]$. [c] The stability constants of the oxidised form of the complex were determined by $\Delta E_{1/2} = (RT/nF)\,[\ln(K_{ML}/K_{ML(ox)})]$, RT/nF having the usual meaning of the Nernst equation.[10]

acid added (see Table 3). After 3 equivalents of acid added no other shift of the oxidation potential was observed, in agreement with the number of protonation constants determined by potentiometry, which is limited by the cavity size and the repulsions between ammonium centres. The shifts observed for L^1 are much lower than those found by Plenio *et al.*[7] for a series of linear and cyclic amines with appended ferrocenyl arms, where the magnitude of the shifts of the redox potentials caused by protonation of the nearby amine was linearly related to the inverse of the Fe–N distance. Based on the linear relationship obtained by those authors for the monoprotonation of amines, a shift of about 190 mV would be expected for the first protonation of L^1. The discrepancy found is a clear indication that the positive charge created by protonation of this compound is not localised on only one nitrogen atom of the macrocycle, but spread over the various centres, and it is a confirmation of the specific sequence of protonation for this compound mentioned before.

The complexation of different metals on the macrocycle of L^1 also shifts the ferrocene–ferrocenium half-wave potential to anodic potentials when compared to that of the free compound, see Table 3. The largest shift is observed in the presence of Cu^{2+}, followed by Ni^{2+}, and then Zn^{2+}, and Cd^{2+}, which is also the indicated order of the decrease of the stability constants. The presence of Pb^{2+} does not result in any shift of the redox potential of L^1, in spite of the relatively stable complex formed (see Table 2). The positive shift of the redox potential by the complexation of metal ions reflects the large decrease of the stability constant of the oxidised complex ML (ox) compared with that of the ML complex, see Table 3.

Another interesting point is that a linear relationship is observed between the current intensity of the ferrocene wave of the complexes and the number of equivalents of metal ion in solution (C_M/C_{L^1}, C_M and C_{L^1} being the total concentrations of the metal ion and L^1, respectively), at a fixed potential. The current decreases when the concentration of the metal ion increases until a 1 : 1 molar ratio is reached. This linear relationship was verified for the Ni^{2+}, Cu^{2+}, Zn^{2+} and Cd^{2+} complexes of L^1, showing a simple method for the quantitative determination of those metals in solution. A similar correlation has previously been observed for the Cu^{2+} complexes of L^{10}.[14]

Of particular importance for evaluating L^1 as a chemical sensor are the results of competition experiments in solution followed by electrochemical techniques; this means the behaviour of the receptor in the presence of several substrates. When an equimolar mixture of Cu^{2+}, Ni^{2+}, Zn^{2+}, Cd^{2+} and Pb^{2+} is added to a solution of L^1 the extent of the anodic shift of the ferrocene–ferrocenium couple is approximately equal to that induced by Cu^{2+} alone. This experiment suggests that L^1 is a copper-selective sensor, which is able to detect copper in the presence of nickel, zinc and cadmium. It is not the first compound for which this property is claimed, but it is probably the easiest and least expensive to synthesize. Indeed, L^9,[9,14] and two polyaza ferrocene macrocyclic ligands,[3] exhibit similar properties. One of these last two compounds presents an even larger value of the anodic shift in the presence of Cu^{2+}, which is not surprising due to the suitable cavity size, modulated by the authors to encapsulate copper selectively, with a suitable number of nitrogen donors and in close position to the ferrocene group.[3] However, it is interesting that the anodic shifts observed for L^9 in the presence of Cu^{2+}, Zn^{2+} and Cd^{2+} are lower than those of L^1 with the same metals and this ligand also exhibits a very low anodic shift in the presence of Ni^{2+}, which is explained by the authors by the geometric arrangement adopted by this complex.[9,14] The relatively good performance of L^1 as a redox sensor can be traced to the presence of the pyridine in the macrocycle and the special geometric arrangements of the macrocycle on complexation with the different metal ions, as will be shown below.

Spectroscopic data in aqueous solution

The copper(II) complex of L^1 in acetonitrile or DMF exhibits a broad band in the visible region due to the copper d–d transitions, and an intense band in the ultraviolet region (*cf.* Table 4). In DMF another band at 438 nm is observed. The EPR spectra are similar in DMF or methanol, exhibiting three well resolved lines at low field and no superhyperfine splitting. The fourth copper line is partially overlapped by the strong and not resolved band of the high field part of the spectra, see Fig. 1. The hyperfine coupling constants and g values of glassy solutions in DMF of $[CuL^1]^{2+}$ and $[CuL^2]^{2+}$, obtained by simulation of the spectra,[30] are compiled in Table 4 together with those of other copper(II) complexes with ligands having the same macrocyclic framework but different arms, taken from the literature.[36,37] Both complexes exhibit three different values of g, and it can be verified that $g_z > (g_x + g_y)/2$, which is typical of the copper(II) ion in rhombic symmetry axially elongated and a $d_{x^2-y^2}$ ground state, consistent with elongated rhombic-octahedral or distorted square-based pyramidal stereochemistries.[23,36–39]

The electronic properties of the Cu^{2+} complexes can be explained by the strength of the axial or equatorial donors and the displacement of the copper atom from the plane of the donor atoms taken from the equations of the EPR parameters derived from ligand field theory.[23,36–41] The addition of axial ligands to a square-planar arrangement has the effect of decreasing A_z and increasing g_z with a simultaneous red shift in the electronic spectra. In agreement with this, it can be observed that $[CuL^3]^{2+}$, which exhibits a square-planar structure as shown by X-ray diffraction analysis,[42] presents lower g_z and higher A_z parameters and its maximum of the visible band is shifted to the blue,[36] when compared with the corresponding values of $[CuL^5]$ (ref. 37) or $[CuL^6]$ (ref. 36), which exhibit octahedral geometry, the nitrogen atoms of the macrocycle forming the equatorial plane and with six-co-ordination completed *via* the two oxygen atoms of the appended carboxylate groups, as also shown by the crystal structure.[37] Therefore, the values of the electronic parameters of these copper complexes are completely consistent with the crystal structures and it can be inferred that they exhibit the same structure in solution and in the solid state.

However, a comparison between the parameters of $[CuL^1]^{2+}$ and those of $[CuL^2]^{2+}$, taken from spectra recorded under the same experimental conditions, reveals a very small increase of g_z, a large increase of A_z and a simultaneous blue shift of the visible band, indicating that those complexes do not follow the behaviour derived from ligand field theory and that other factors need to be considered. Actually, these results give a clear indication of a geometrical distortion of the planar to tetrahedral geometry in the case of $[CuL^1]^{2+}$, as the EPR parameters are very sensitive to this geometrical distortion, the variations

Table 4 Spectroscopic and EPR data for the Cu^{2+} complexes of L^1 and similar complexes

Complex	Visible band, λ/nm (ε/dm^3 mol^{-1} cm^{-1})	EPR parameters (10^4 A_i/cm^{-1})						Ref.
		g_x	g_y	g_z	A_x	A_y	A_z	
$[CuL^1]^{2+}$	600 (254.7) in DMF	2.032	2.074	2.199	0.8	17.2	170.3	*a*
$[CuL^2]^{2+}$	560 (236.8) in DMF 550 (119) in water	2.039	2.080	2.201	4.9	14.7	195.9	*a*
$[CuL^3]^{2+}$	560 (187) in water	2.034	2.060	2.188	0.5	3.4	192.9	*b*
$[CuL^5]$	614 (103.9) in water	2.034	2.080	2.209	14.3	8.5	167.1	*c*
$[CuL^6]$	630 (97.1) in water	2.027	2.084	2.221	14.9	21.3	165.4	*b*

[a] This work. [b] Ref. 37. [c] Ref. 36.

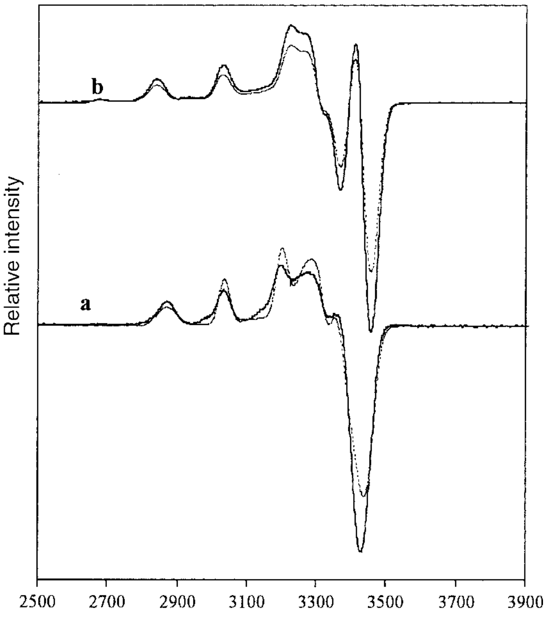

Fig. 1 EPR X-band spectra of the Cu^{2+} complexes of L^1 (a) and L^2 (b) in DMF, recorded at 115 K, microwave power 2.4 mW, modulation amplitude 1.0 mT. The frequency (ν) was 9.614 and 9.615 GHz for (a) and (b), respectively.

in A_z being very large.[43] These conclusions are consistent with the structure determined in the solid state, as shown below, and confirm that the structures in solution and in the solid state are similar.

Table 5 Room temperature crystal data and pertinent refinement parameters for metal complexes **1** and **2**

	1	**2**
Empirical formula	$C_{72}H_{90.5}Cl_3Cu_2Fe_4IN_8O_{1.25}$	$C_{36}H_{46}ClFe_2IN_4O_2Zn$
M	1671.75	906.19
Crystal system	Triclinic	Monoclinic
Space group	$P\bar{1}$	*C*2/*c*
a/Å	12.292(14)	41.984(45)
b/Å	17.784(19)	10.348(13)
c/Å	19.347(23)	18.951(22)
α/°	92.31(1)	
β/°	96.64(1)	107.62(1)
γ/°	108.04(1)	
V/Å^3	3981(8)	7847(16)
Z	2	8
μ/mm^{-1}	1.767	2.226
Reflections measured	13980	5034
Unique reflections	13980 (R_{int} = 0.0000)	3644 (R_{int} = 0.0814)
R and R_w [$I > 2\sigma(I)$]	0.0967, 0.2597	0.0899, 0.2287
(all unique data)	0.1595, 0.3011	0.2573, 0.2911

Crystallographic structural studies

The crystal structures of $[CuL^1Cl][CuL^1I]Cl_2\cdot1.25H_2O$ **1** and $[ZnL^1I]Cl\cdot2H_2O$ **2** were determined using single crystal X-ray diffraction analysis (Table 5). The chemical identity of the halogen atoms in the three complexes was investigated carefully considering all possible combinations between chlorine and iodine atoms in the successive trial refinements. Therefore the molecular formulation presented in each case corresponds to the combination with low *R* values and low anisotropic thermal parameters for chlorine and/or iodine atoms. The molecular formulations found by X-ray diffraction for both complexes are consistent with the other experimental data.

The X-ray study for compound **1** showed that two different copper complexes $[CuL^1Cl]^+$ (see below) and $[CuL^1I]^+$ compose the asymmetric unit of this complex. The two discrete anions required by charge balance were identified as chlorides, which are disordered and located in eight alternative positions, two of them in close proximity. The occupancies of these two positions were set arbitrarily to 0.30 and 0.20 respectively. The remaining six are spread in the unit cell, each with occupancy of 0.25. One water molecule displays an occupancy of 0.5 and, for the remaining three, occupancies of 0.25 were assigned.

The crystal structure of complex **2** is built up from an asymmetric unit composed of one cation $[ZnL^1I]^+$ $\mathbf{2}^+$ and one anion Cl^- and four water molecules with different occupancies. One of the water molecules as well as the Cl^- anion are disordered over two sites in the crystal lattice. Refined occupancies of 0.75(2) and 0.25(2) for Cl^- and 0.72(5) and 0.28(5) for the water molecule were found. The remaining three water molecules are spread in the unit cell, two with occupancies of 0.25 and one with an occupancy of 0.50. Therefore, the molecular formula $[ZnL^1I]Cl\cdot2H_2O$ was established by X-ray diffraction.

Complex **3** was also investigated by X-ray single crystal diffraction. Unfortunately the compound in the solid state was composed of *ca.* 50% of crystal and *ca.* 50% of powder and displayed a very poor diffraction pattern. In fact the image plate pictures taken of the X-ray diffraction pattern from different crystals showed that they had a low degree of crystallinity. However it was possible to solve the structure of this compound, all non-hydrogen atoms have been located unambiguously and their positions refined with anisotropic thermal parameters. In spite of this the final quality of the crystal structure is not enough for publication, but the dimensions associated with the metal co-ordination spheres are accurate enough to be included in a broader discussion of conformational features associated with the flexible framework of macrocycle L^1 in the metal transition complexes.[44]

The cations in the complexes studied show the metal to be five-co-ordinated and display a [4 + 1] co-ordination type. For comparison their structures will be discussed together. Molecular diagrams including the atomic notation schemes are presented in Fig. 2 for complexes $[CuL^1Cl]^+$ $\mathbf{1a}^+$ and $[CuL^1I]^+$ $\mathbf{1b}^+$ and in Fig. 3 for complex $[ZnL^1I]^+$ $\mathbf{2}^+$. The bond lengths and angles subtended at the metal centres, listed in Table 6, indicate that the three complex cations have distorted square pyramidal co-ordination spheres. The basal planes are

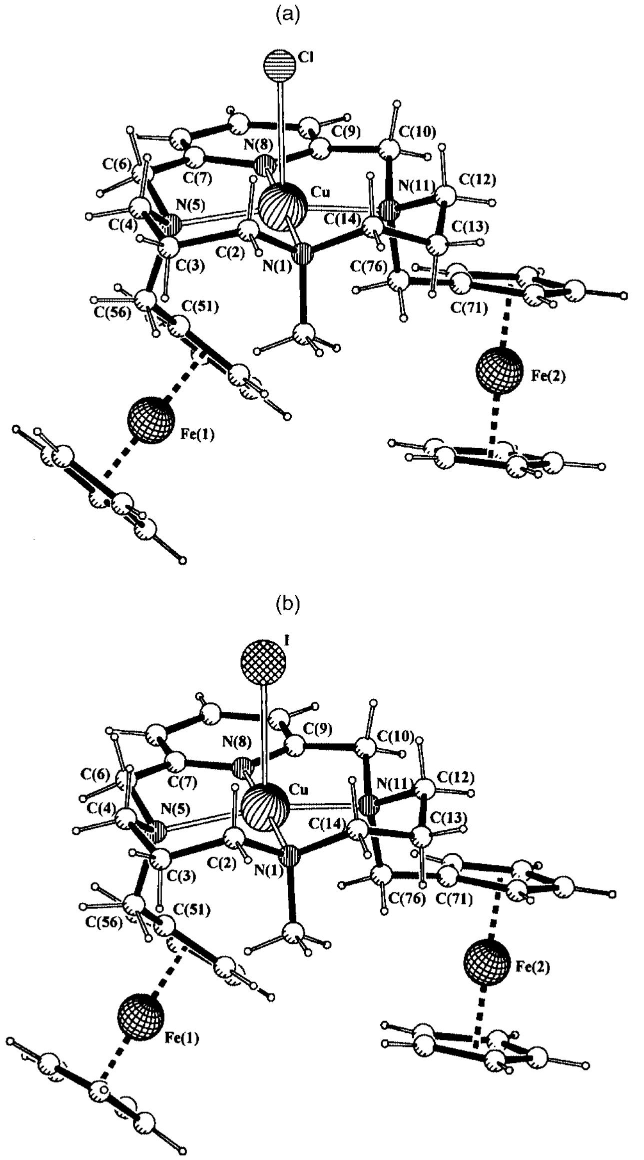

Fig. 2 PLUTON views of the copper(II) complexes of L^1 showing their molecular geometries and the atomic notation scheme adopted: (a) $[CuL^1Cl]$ **1a**$^+$ and (b) $[CuL^1I]$ **1b**$^+$. For clarity only the atomic notation for the quoted atoms in the text is included.

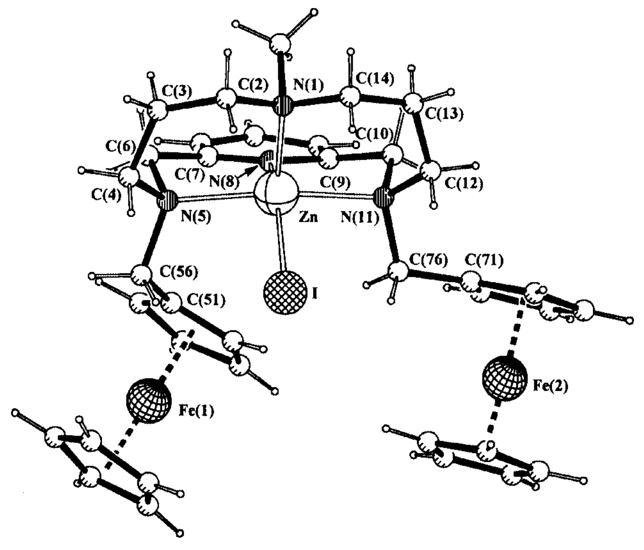

Fig. 3 A PLUTON view of $[ZnL^1I]$ **2**$^+$. Details as in Fig. 2.

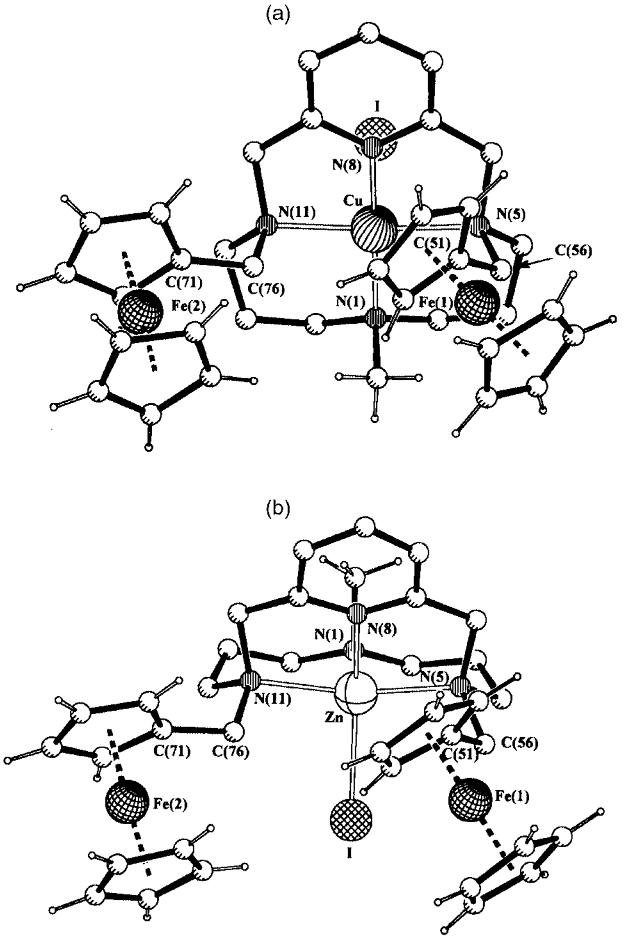

Fig. 4 Views of $[CuL^1I]$ **1b**$^+$ (**a**) and $[ZnL^1I]$ **2**$^+$ (**b**) complexes, perpendicular to the basal plane, illustrating the different spatial orientation of the two Cp_2Fe redox units relatively to the metal receptor site.

formed by the four nitrogen atoms of the macrocycle in **1a**$^+$ and **1b**$^+$ while in **2**$^+$ it is defined by three nitrogen atoms of L^1 and one iodine atom. The apical positions are occupied by the nitrogen donor atom of the macrocycle *trans* to the pyridine ring in complex **2**$^+$ and by a chlorine atom in **1a**$^+$ and by an iodine atom in **1b**$^+$. The complex $[NiL^1Cl]^+$ **3**$^+$ has an overall geometry comparable to that found for **2**$^+$ with the iodine atom replaced by a chlorine. To achieve the geometric arrangement described for **2**$^+$, the macrocycle L^1 folds considerably through the line defined by the nitrogen atoms N(5) and N(11) leading a dihedral angle between the planes [N(8), N(5), N(11)] and [N(1), N(5), N(11)] of 73.7(9) in **2**$^+$ and 79.6(7)° in **3**$^+$.

The two ferrocenyl units (Cp_2Fe) and N-methyl group are on the same side of the N_4 macrocyclic plane in complex **1a**$^+$ and **1b**$^+$ while in **2**$^+$ and **3**$^+$ the methyl group is on the opposite side to the two Cp_2Fe units. However the two Cp_2Fe units display different spatial orientations leading to different distances between the metal centres, Cu^{II}, Ni^{II} or Zn^{II}, and the Cp_2Fe redox units. The intramolecular distances between the Cp_2Fe groups and the metal centres as well as selected exocyclic torsion angles are given in Table 7. In all complex cations the N(5)–C(56) and N(11)–C(76) bonds display *gauche* and *trans* conformations, respectively. Consequently Fe(1)···M distances much shorter than those of Fe(2)···M were found for all complexes. These intramolecular dimensions as well as the Fe···Fe distances (see Table 7) should be relevant for understanding the behaviour of the complexes as redox sensors, if the same conformations are kept in solution (see below). The different orientations of the two Cp_2Fe units relatively to the receptor site are illustrated in Fig. 4 for complexes **1b**$^+$ and **2**$^+$. Furthermore the two Cp_2 units adopt an eclipsed orientation in complexes **2**$^+$ and **1b**$^+$ while in **1a**$^+$ and **3**$^+$ they exhibit staggered and eclipsed orientations, respectively.

The Cu–Cl distance of 2.855(6) Å in complex **1a**$^+$ is on the long side of distances reported for five-co-ordinated complexes containing $CuClN_4$ co-ordination spheres, which range between 2.364 and 2.736 Å.[45] On the other hand there are in the literature many structures, with chlorine bridges or with chlorines in axial positions of an octahedron, having longer Cu–Cl distances *ca.* 3.0 Å.[45] Furthermore, the angles centred at the copper involving the chlorine atom (see Table 6) are consistent with a distorted square pyramidal geometric arrangement of [4 + 1] type with the apical position occupied by the halogen atom. In other words, a weak bond between the copper and the chlorine atom is suggested. The Cu–I distance of 2.931(3) Å in **1a**$^+$ is in the range of distances, 2.587–3.031 Å, found for copper five-co-ordinated complexes with an IN_4 atom donor set.

The two copper complexes contain very similar Cu–N bond lengths and N–Cu–N angles in the basal plane. The distance Cu–N(py) to the nitrogen atom of the pyridine [Cu–N(8) 1.921(10) Å in **1a**$^+$ and 1.928(7) Å in **1b**$^+$] is shorter than those found for the remaining three tertiary nitrogen atoms [average values 2.096(10) Å in **1a**$^+$ and 2.095(9) Å in **1b**$^+$]. The best least-squares plane through the nitrogen atoms exhibits a small tetrahedral distortion of ±0.158(4) and ±0.149(4) Å for **1a**$^+$ and **1b**$^+$, respectively. The copper lies out of the N_4 plane by 0.195(4) in **1a** and 0.230(4) Å in **1b** towards the apical ligand. Arrangements with similar geometric parameters on the equatorial plane were found for the square planar complex $[CuL^3]^{2+}$ **4** (ref. 42) and the five-co-ordinated complex $[CuL^2(NO_3)]^+$ **5** (ref. 46), in which the apical position is filled by the NO_3 ligand. The Cu–N sp^2 distance and the average Cu–N sp^3 distances are respectively 1.904(8) and 2.015(8) Å in **4** and 1.934(2) and 2.027(2) Å in **5**.

Table 6 Bond lengths (Å) and angles (°) in the co-ordination sphere of the complex cations **1a**$^+$, **1b**$^+$ and **2**$^+$

	1a$^+$ [M = Cu^{II}]	**1b**$^+$ [M = Cu^{II}]	**2**$^+$ [M = Zn^{II}]
Equatorial	[X = N(1)]	[X = N(1)]	(X = I)
M–X	2.012(10)	2.006(9)	2.610(4)
M–N(5)	2.131(10)	2.130(9)	2.176(17)
M–N(8)	1.921(10)	1.928(7)	2.146(17)
M–N(11)	2.146(10)	2.149(8)	2.230(17)
N(8)–M–X	177.8(3)	175.3(3)	148.5(5)
N(5)–M–N(11)	154.8(4)	153.1(3)	150.3(7)
N(5)–M–X	97.7(4)	97.7(4)	97.4(6)
N(8)–M–N(5)	82.6(4)	81.7(3)	78.5(7)
N(8)–M–N(11)	81.0(4)	80.4(3)	75.6(8)
N(11)–M–X	98.0(4)	98.5(4)	97.1(5)
Apical	(Y = Cl)	(Y = I)	[= N(1)]
M–Y	2.855(6)	2.931(3)	2.060(20)
X–M–Y	94.1(3)	97.0(3)	104.9(7)
N(5)–M–Y	97.6(3)	101.0(2)	101.6(9)
N(8)–M–Y	88.0(3)	87.7(2)	106.5(9)
N(11)–M–Y	100.8(2)	98.2(2)	99.5(9)

The co-ordination sphere of complex **2**$^+$ is strongly distorted. The N_3I equatorial plane shows a small tetrahedral distortion of ±0.111(9) Å, but the metal is significantly out of this plane by 0.525(9) Å. Furthermore, the Zn–N(1) distance of 2.060(20) Å, involving the nitrogen atom *trans* to the pyridine, is the shortest of the Zn–N bond lengths found. This structural feature is striking since it does not follow the usual bond length pattern of the metal complexes of macrocycles containing pyridine, as found for the copper(II) complexes of L^1 reported in this study, as well as for $[NiL^1Cl]^+$ **3**$^+$ [Ni–N(py) 1.975(21) and average Ni–N sp^3 2.126(20) Å],[44] and for other related nickel complexes: $[NiL^4Cl]^+$ **6** (ref. 47), $[NiL^4(dmso)]^{2+}$ **7** (ref. 47) and $[NiL^4(H_2O)]^{2+}$ **8** (ref. 48) which display also folded geometric arrangements with the fifth position occupied by the monodentate ligand. The usual bond length pattern is also observed in the two related five-co-ordinated zinc(II) complexes available from the literature, $[ZnL^7]^{2+}$ **9** (ref. 49) and $[ZnL^8]^{2+}$ **10** (ref. 50). The Zn–N distance involving the pyridine ring of the macrocycle is 2.018(8) Å in **9** and 2.012(6) Å in **10** while the remaining three Zn–N distances are 2.198(9), 2.188(9) and 2.091(8) Å in **9** and 2.229(7), 2.261(6), 2.073(7) Å in **10**. These two complexes show a strongly distorted square pyramidal geometry, with the basal plane defined by the four nitrogen atoms of the macrocycle and the apical position occupied by the nitrogen of the pyridyl pendant arm. The N-pyridyl arm and the two N–H hydrogen atoms in **9** or the two benzyl groups in **10** are on the same side of the N_4 macrocyclic plane leading to a conformation which is different from that described for $[ZnL^1I]^+$. Therefore, the macrocycle has enough flexibility to provide two conformations with different cavity sizes suitable for the co-ordination of Zn^{II}, the folded one adopted by L^1 in **2** exhibiting larger steric constraints and causing pronounced bond length distortions in this complex. The presence of bulky groups, such as benzyl or ferrocenyl, introduces also a remarkable degree of deviation in the Zn–N distances, as can be seen by comparison of the distances of **2** with those of **9** and **10**.

The conformations adopted by the parent macrocycle L^2, and its N-methyl derivatives, in the transition metal complexes have been described in terms of the positions of the N-substituent group relative to the macrocyclic ring.[42] The + and − signs indicate that these groups are located above or below the macrocycle, respectively. Following this nomenclature, L^1 exhibits a conformation called − − −a in the present two copper complexes, since the two N-ferrocenyl groups and the N-methyl group are positioned below the N_4 basal co-ordination plane and opposite the apical ligand, the chlorine or the iodine atom. In the nickel and zinc complexes, the macrocycle displays a folded conformation + − +e, in which the N-methyl and two ferrocenyl groups are on opposite sides of the macrocyclic ring. Furthermore, in this form the monodentate ligand in equatorial position is on the same side as the two ferrocenyl groups. To describe precisely the position of the fifth donor atom in the metal co-ordination sphere, *a* (axial) and *e* (equatorial) labels are used. The two different conformations are illustrated in Fig. 4.

In order to compare the conformations exhibited by the complexes of L^1 under study with those adopted by the parent

Table 7 The intramolecular distances (Å) between the Cp_2Fe redox centres and the metal receptors (M) and selected exocyclic torsion angles (°)

	1a$^+$	**1b**$^+$	**2**$^+$	**3**$^+$
	M = Cu^{II}	M = Cu^{II}	M = Zn^{II}	M = Ni^{II}
Fe(1) · · · Fe(2)	6.655(6)	6.678(8)	7.015(8)	6.935(8)
Fe(1) · · · M	5.350(6)	5.396(5)	5.347(7)	5.239(6)
Fe(2) · · · M	6.138(6)	6.149(5)	6.120(8)	6.112(9)
M–N(5)–C(56)–C(51)	−49.8(11)	−52.0(11)	−67.1(21)	−52.0(29)
M–N(11)–C(76)–C(71)	163.7(7)	171.2(7)	−179.2(12)	−165.1(16)

Table 8 Endocyclic torsion angles (°) in the macrocyclic framework of L^1, L^2 and L^3 in the five-co-ordinated complexes[a]

Complex	N(1)–C(2)	C(2)–C(3)	C(3)–C(4)	C(4)–N(5)	N(5)–C(6)	C(6)–C(7)	C(7)–N(8)	N(8)–C(9)	C(9)–C(10)	C(10)–N(11)	N(1)–C(12)	C(12)–C(13)	C(13)–C(14)	C(14)–N(1)
1a$^+$ [CuL^{1}Cl]$^{+b}$	−175.8(12)	−69.5(16)	68.2(15)	−172.5(12)	146.9(11)	−26.2(15)	175.3(10)	169.8(10)	35.8(13)	−159.5(10)	168.0(11)	−72.1(14)	79.9(15)	−179.5(12)
1b$^+$ [CuL^{1}I]$^{+b}$	−179.9(11)	−68.5(15)	67.2(14)	−169.6(10)	149.7(9)	−28.8(11)	171.3(8)	−171.5(8)	31.5(10)	−156.8(8)	167.6(10)	−68.2(14)	71.8(14)	−175.8(10)
5 [CuL^2(NO$_3$)]$^{+c}$	−178.3	−67.5	68.3	172.3	145.5	−16.3	179.1	−179.6	21.5	−157.8	178.9	−67.4	71.7	−177.6
11 [NiL^2(ClO$_4$)]$^{+d}$	−175.0	−68.3	64.7	176.9	165.6	−25.4	172.6	−172.3	17.1	−151.6	173.1	−64.7	70.6	−177.6
2$^+$ [ZnL^{1}I]$^{+b}$	−176.6(24)	60.8(37)	−60.8(35)	−73.3(28)	153.5(21)	−34.7(31)	−175.3(22)	170.8(25)	35.1(31)	−152.2(18)	73.5(24)	63.0(29)	−61.8(34)	179.1(22)
3$^+$ [NiL^{1}Cl]$^{+b}$	−165.8(22)	66.3(42)	−63.7(49)	−72.4(37)	148.7(25)	−27.0(39)	−175.3(21)	173.0(23)	34.5(30)	−154.8(26)	56.0(41)	76.7(41)	−73.1(31)	175.4(21)
6 [NiL^{4}Cl]$^{2+e}$	−178.3	73.8	−66.7	−71.6	151.8	−25.6	−175.3	174.4	27.5	−153.3	71.3	65.7	−71.6	175.8
7 [NiL^4(dmso)]$^{2+e}$	−179.6	76.5	−73.4	−60.1	156.1	−35.4	−168.3	177.7	22.4	−149.1	71.1	62.7	−63.8	167.6
8 [NiL^4(H$_2$O)]$^{2+f}$	−176.8	70.9	−62.7	−73.1	152.8	−24.9	−177.8	175.7	23.3	−151.5	77.3	65.6	−74.6	178.1

[a] The bond lengths quoted represent the middle bond of the corresponding endocyclic torsion angle and the bonds are labelled using the atomic notation scheme presented in Figs. 2 and 3 for the studied complexes. [b] This work. [c] Ref. 46. [d] Ref. 42. [e] Ref. 47. [f] Ref. 48.

L^2 and its N-alkyl derivatives in five-co-ordinated transition metal complexes, a search on the Cambridge Data Base was carried out.[45] In Table 8 are listed the complexes, their sources, and the endocyclic torsion angles found for the framework of the macrocycles. The X-ray data available include only three complexes of L^4 and two of L^2. As is also found in the nickel and zinc complexes of L^1, the three nickel complexes of L^4 exhibit a +−−+e folded arrangement while the copper and nickel complexes of L^2 show a −−−a planar arrangement comparable to that found for the two copper complexes of L^1. Therefore there are only two different sets of complexes, one having +−−+e and the other with a −−−a conformation. On the other hand the complexes in each set have comparable endocyclic torsion angles indicating that the number and the type of N-substituents (bulky or not) has little influence on the conformation of the macrocyclic framework. Furthermore the structures presented in this study of L^1 with Cu, Zn and Ni, namely **1b**$^+$, **2**$^+$ and **3**$^+$, offer the possibility of tracing a relationship between the ion size and the conformation adopted by this macrocycle in a square pyramidal geometric environment.

A detailed study of the conformational preferences of L^3 and L^4 in four- and five-co-ordinated metal transition complexes was carried out by molecular mechanics calculations (MM).[42] Values of the steric energy *versus* M–N distance were calculated for L^3 with the metal ion in a five-co-ordinate environment indicated that for distances M–N up to 2.15 Å there are three preferred forms, having in common an axial monodentate ligand. The most stable conformation up to M–N distances of ≈1.9 Å is +++a, followed by −++a between 1.9 and 2.05 Å and −−−a between 2.05 and 2.15 Å. The equatorial +−−+e form is favoured for distances longer than 2.15 Å. When the three N–H hydrogen atoms in L^3 were replaced by three methyl groups to give L^4 more interesting results were found. The +−−+e equatorial form becomes more stable in the complete range of the distances studied, but barely distinguishable from the −−−a near their minima, between 1.95 and 2.15 Å. The structural preferences based on the steric constraints of L^4 are consistent with the geometries found for copper, nickel, and zinc complexes of L^1. The average M–N distances [Cu^{II}–N 2.05 Å in **1a**$^+$ and **1b**$^+$, Zn^{II}–N 2.15 Å in **2**$^+$ and Ni^{II}–N 2.09 Å in **3**$^+$] are within the range where the equatorial +−−+e and axial −−−a arrangements of L^4 have similar steric stability.

In conclusion the MM results in the gas phase as well as the crystal structures show that N-substituents with very different steric requirements, such as hydrogen atoms, methyl or bulky ferrocenyl groups, do not determine the conformation exhibited by the macrocycle in its transition metal complexes. Instead, this seems more a result of a delicate balance between the electronic and geometric preferences of the transition metal ion and the steric constraints of the macrocyclic frameworks of L^1–L^4. Furthermore the match between the size of ion and the size the macrocyclic cavity plays also an important role in the recognition process between the host (the macrocycle) and the guest (the metal). Thus the flexible folded conformation +−−+e is favoured for the metals of larger sizes even in strongly distorted geometric environments, as found for example for the zinc(II) complex of L^1. However this conformation can be adopted by the macrocycle in the co-ordination of small metal ions, such as Ni^{II}, as reported for complexes of this metal with L^1 and L^4. By contrast the conformation −−−a is preferred only when co-ordinated to small ions as Cu^{II} with L^1 and L^4 or Ni^{II} with L^2.

Conclusion

The steric hindrance of the bulky N-ferrocenyl appended arms in the macrocycle L^1 disturbs the protonation sequence of this compound rendering it more acidic than the parent macrocycle, L^2.

The electrochemical behaviour of L^1 clearly indicates that this redox-active compound is a selective sensor for copper in environments containing late transition metals such as nickel, zinc or cadmium. Furthermore the anodic shifts of the ferrocene–ferrocenium redox potential of L^1 with the metal ions studied are different, so that copper has the higher value, followed immediately by nickel, and zinc and cadmium exhibit lower values. These results contrast with the crystal structures obtained for the five-co-ordinated copper, nickel and zinc complexes. While in the copper(II) complex the macrocycle adopts the planar $---$a conformation, the nickel(II) and zinc(II) complexes exhibit the folded $+--+$e conformation, and the discussion above, based on an MM study, suggests that the cadmium complex also adopts the folded $+--+$e conformation. In spite of the structures showing that the nickel complex in the solid state displays the folded conformation, MM calculations indicate that the $---$a conformation is also a favoured arrangement for this metal. Therefore, the electrochemical behaviour of L^1 in the presence of this metal, more similar to that of copper than zinc, can be explained in terms of an equilibrium between the $+--+$e and $---$a forms in solution.

The flexibility of the macrocycle framework plays an important role in the complexing ability of L^1 and consequently in its behaviour as a redox sensor. Indeed, our results emphasise the relevance of the conformation adopted by the macrocycle and the spacial orientation of the ferrocenyl arms in the transition metal complexes in its electrochemical behaviour. For the more covalently bonded complexes studied in this work it is not straightforward to establish a linear relationship either between the redox shift ($\Delta E_{1/2}$) *versus* the charge-to-size ratio as found for alkali or alkaline-earth metals[2] or *versus* the reciprocal distance between the alkali metal (Na$^+$) and the redox centre (Na$^+$–Fe distance).[8] However, in spite of the large intramolecular distances between the ferrocene groups and the transition metal centres studied in this work (Table 7), they show different values in the three complexes which are consistent with the redox shift exhibited by L^1 in the presence of the Ni^{2+}, Cu^{2+} and Zn^{2+}. In other words these distances seem to have a crucial relevance in the redox behaviour of these complexes.

Acknowledgements

The authors acknowledge the financial support of Fundação para a ciência e tecnologia and PRAXIS XXI (Project n. PRAXIS/2/2.1/QUI/316/94). We thank the EPSRC (UK) and the University of Reading for funds for the Image Plate System and Mrs A. W. Johans for his assistance with the crystallography. The authors also thank Carla Gamelas for the synthesis of (ferrocenylmethyl)trimethylammonium iodide.

References

1 P. D. Beer, *Chem. Soc. Rev.*, 1989, **18**, 409.
2 J. C. Medina, T. T. Goodnow, M. T. Rojas, J. L. Atwood, B. C. Lynn, A. E. Kaifer and G. W. Gokel, *J. Am. Chem. Soc.*, 1992, **114**, 10583.
3 P. D. Beer, Z. Chen, M. G. B. Drew, J. Kingston, M. Ogden and P. Spencer, *J. Chem. Soc., Chem. Commun.*, 1993, 1046.
4 H. Plenio, H. El-Desoky and J. Heinze, *Chem. Ber.*, 1993, **126**, 2403.
5 C. D. Hall, in *Ferrocene-Homogeneous Catalysis. Organic Synthesis. Material Sciences*, eds. A. Togni and T. Hayashi, VCH, New York, 1994, pp. 279–316.
6 P. D. Beer, Z. Chen, M. G. B. Drew and A. J. Pilgrim, *Inorg. Chim. Acta*, 1994, **225**, 137.
7 H. Plenio, J. Yang, R. Diodone and J. Heinze, *Inorg. Chem.*, 1994, **33**, 4098.
8 H. Plenio and R. Diodone, *Inorg. Chem.*, 1995, **34**, 3964.
9 M. J. L. Tendero, A. Benito, J. Cano, J. M. Loris, R. Martinez-Máñez, J. Soto, A. J. Edwards, P. R. Raithby and M. A. Rennie, *J. Chem. Soc., Chem. Commun.*, 1995, 1643.
10 M. J. L. Tendero, A. Benito, R. Martinez-Máñez, J. Soto, J. Payà, A. J. Edwards and P. R. Raithby, *J. Chem. Soc., Dalton Trans.*, 1996, 343.
11 M. J. L. Tendero, A. Benito, R. Martinez-Máñez, J. Soto, E. García-España, J. A. Ramírez, M. I. Burguete and S. V. Luis, *J. Chem. Soc., Dalton Trans.*, 1996, 2923.
12 M. J. L. Tendero, A. Benito, R. Martinez-Máñez and J. Soto, *J. Chem. Soc., Dalton Trans.*, 1996, 4121.
13 H. Plenio and C. Aberle, *Organometallics*, 1997, **16**, 5950.
14 J. M. Lloris, R. Martinez-Máñez, T. Pardo, J. Soto and M. E. Padilla-Tosta, *J. Chem. Soc., Dalton Trans.*, 1998, 2635.
15 P. D. Beer and D. K. Smith, *J. Chem. Soc., Dalton Trans.*, 1998, 417.
16 J. M. Lloris, R. Martinez-Máñez, M. E. Padilla-Tosta, T. Pardo, J. Soto, E. García-España, J. A. Ramírez, M. I. Burguete, S. V. Luis and E. Sinn, *J. Chem. Soc., Dalton Trans.*, 1999, 1779.
17 P. D. Beer, D. B. Crowe, M. I. Ogden, M. G. B. Drew and B. Main, *J. Chem. Soc., Dalton Trans.*, 1993, 2107.
18 P. D. Beer, M. G. B. Drew, J. Hodacova and S. E. Stokes, *J. Chem. Soc., Dalton Trans.*, 1995, 3447.
19 P. D. Beer, *Chem. Commun.*, 1996, 689.
20 J. M. Lloris, R. Martinez-Máñez, M. E. Padilla-Tosta, T. Pardo, J. Soto and M. J. L. Tendero, *J. Chem. Soc., Dalton Trans.*, 1998, 3659.
21 P. D. Beer, *Acc. Chem. Res.*, 1998, **31**, 71.
22 K. P. Balakrishnan, H. A. A. Omar, P. Moore, N. W. Alcock and G. A. Pike, *J. Chem. Soc., Dalton Trans.*, 1990, 2965.
23 J. Costa and R. Delgado, *Inorg. Chem.*, 1993, **32**, 5257.
24 D. Lednicer and C. R. Hauser, *Org. Synth.*, 1960, **40**, 31.
25 M. C. Grossel, D. G. Hamilton, J. I. Fuller and E. Millan-Barios, *J. Chem. Soc., Dalton Trans.*, 1997, 3471.
26 J. Costa, R. Delgado, M. G. B. Drew and V. Félix, *J. Chem. Soc., Dalton Trans.*, 1999, 4331.
27 G. Gran, *Analyst* (*London*), 1952, **77**, 661; F. J. Rossotti and H. J. Rossotti, *J. Chem. Educ.*, 1965, **42**, 375.
28 C. H. Rochester, *J. Chem. Soc., Dalton Trans.*, 1972, 5.
29 P. Gans, A. Sabatini and A. Vacca, *Talanta*, 1996, **43**, 1739.
30 F. Neese, Diploma Thesis, University of Konstanz, June 1993.
31 I. V. Nelson and R. T. Iwamoto, *Anal. Chem.*, 1963, **35**, 867.
32 W. Kabasch, *J. Appl. Crystallogr.*, 1988, **21**, 916.
33 N. Walker and D. Stuart, DIFABS, *Acta Crystallogr., Sect. C*, 1983, **39**, 158.
34 G. M. Sheldrick, SHELX 97, University of Göttingen, 1997.
35 A. L. Spek, PLATON, a Multipurpose Crystallographic Tool, Utrecht University, 1999.
36 J. Costa, R. Delgado, M. C. Figueira, R. T. Henriques and M. Teixeira, *J. Chem. Soc., Dalton Trans.*, 1997, 65.
37 J. Costa, R. Delgado, M. G. B. Drew and V. Félix, *J. Chem. Soc., Dalton Trans.*, 1998, 1063.
38 B. J. Hathaway, *Coord. Chem. Rev.*, 1983, **52**, 87.
39 H. Yokoi, M. Sai, T. Isobe and S. Ohsawa, *Bull. Chem. Soc. Jpn.*, 1972, **45**, 2189.
40 P. W. Lau and W. C. Lin, *J. Inorg. Nucl. Chem.*, 1975, **37**, 2389.
41 M. J. Maroney and N. J. Rose, *Inorg. Chem.*, 1984, **23**, 2252.
42 V. Félix, M. J. Calhorda, J. Costa, R. Delgado, C. Brito, M. T. Duarte, T. Arcos and M. G. B. Drew, *J. Chem. Soc., Dalton Trans.*, 1996, 4543.
43 I. Bertini, G. Canti, R. Grassi and A. Scozzafava, *Inorg. Chem.*, 1980, **19**, 2198.
44 Complex [NiL^{1}Cl]Cl **3** crystallises in the monoclinic system, space group $P2_1/c$ with $a = 17.207(22)$, $b = 11.537(16)$, $c = 18.546(21)$ Å, $\beta = 95.43(1)°$. A final refinement of 348 parameters led to $R = 0.1662$, $R' = 0.4149$ for 1620 observed reflections with $I > 2\sigma(I)$. M. G. B. Drew and V. Félix, unpublished work.
45 F. H. Allen, J. E. Davies, J. J. Galloy, O. Johnson, O. Kennard, C. F. Macrae and D. G. Watson, *J. Chem. Inf. Comput. Sci.*, 1991, **31**, 204.
46 T.-H. Lu, S.-F. Tung, T.-Y. Chi and C.-S. Chung, *Acta Crystallogr., Sect. C*, 1998, **54**, 1069.
47 N. W. Alcock, P. Moore and H. A. A. Omar, *J. Chem. Soc., Dalton Trans.*, 1987, 1107.
48 K. A. Foster, E. K. Barefield and G. Van Derver, *J. Chem. Soc., Dalton Trans.*, 1986, 680.
49 S. J. Grant, P. Moore, H. A. A. A. Omar and N. W. Alcock, *J. Chem. Soc., Dalton Trans.*, 1994, 485.
50 N. W. Alcock, K. P. Balakrishnan, A. Berry, P. Moore and C. J. Reader, *J. Chem. Soc., Dalton Trans.*, 1988, 1089.